Available online at www.sciencedirect.com
ScienceDirect
Journal of Power Sources 179 (2008) 69–80
JOURNAL OF POWER SOURCES
www.elsevier.com/locate/jpowsour

# Synthesis and characterization of polyvinyl alcohol copolymer/phosphomolybdic acid-based crosslinked composite polymer electrolyte membranes

Arfat Anis [a,*], A.K. Banthia [a], S. Bandyopadhyay [b]

[a] *Materials Science Centre, Indian Institute of Technology, Kharagpur, India*
[b] *School of Materials Science & Engineering, University of New South Wales, Sydney, Australia*

Received 1 November 2007; received in revised form 10 December 2007; accepted 10 December 2007
Available online 23 December 2007

**Abstract**

Polymer electrolyte membrane fuel cells (PEMFCs) are very promising as future energy source due to their high-energy conversion efficiency and will help to solve the environmental concerns of energy production. Polymer electrolyte membrane (PEM) is recognised as the key element for an efficient PEMFC. Chemically crosslinked composite membranes consisting of a poly(vinyl alcohol-co-vinyl acetate-co-itaconic acid) (PVACO) and phosphomolybdic acid (PMA) have been prepared by solution casting and evaluated as proton conducting polymer electrolytes. The proton conductivity of the membranes is investigated as a function of PMA composition, crosslinking density and temperature. The membranes have also been characterized by FTIR spectroscopy, TGA, AFM and TEM. The proton conductivity of the composite membranes is of the order of $10^{-3}$ S cm$^{-1}$ and shows better resistance to methanol permeability than Nafion 117 under similar measurement conditions.


*Keywords:* Fuel cells; Polymer electrolyte membrane; Polyvinyl alcohol; Phosphomolybdic acid; Proton conductivity; Methanol permeability

## 1. Introduction

Proton conducting polymer electrolyte membranes are of interest for a broad range of applications, such as biosensors, chemical sensors, catalysts, actuators, ion-exchange membranes and polymer electrolyte membrane (PEM) fuel cells [1–5]. PEM fuel cells have attracted considerable attention as a promising source of electrical power for transportation, residential and portable applications due to their high efficiency and clean production.

As a proton conducting membrane, perfluorinated ionomers have been the most widely used material for fuel cell operations. There has been a great demand for alternative proton conducting membranes for DMFC due to the methanol crossover problem associated with the perfluorinated membranes together with the high cost and environmental inadaptability of these membranes. Several methods have been proposed for the development of alternative membranes, and promising results have been obtained with the use of composite membranes, where inorganic particles are embedded into a polymer matrix [6–9]. Herring et al. and Ramani et al. have reported that the proton conductivity and durability of the perfluorosulfonic acid (PFSA) ionomers and fuel cell performance of membrane electrode assemblies (MEA) can be improved by the addition of heteropoly acids (HPAs) [10–13]. The HPAs, a subset of the polyoxometallates, are an extensive class of structurally well-defined inorganic metal oxide clusters that contain a central heteroatom [14]. These superacidic inorganic oxides are synthetically versatile, exhibit redox catalyst activity, and have very high proton conductivity in the solid state. These are known to have strong interactions with the sulfonic acid groups of ionomers [15] into which they are doped, resulting in morphological changes, as compared with the undoped ionomers. The HPAs are becoming an increasingly popular proton conducting additives in ionomer composite membranes for use under dry and/or elevated temperature conditions [16].

However, the HPAs are water-soluble materials and may leach out of the membranes; which would result in declining

* Corresponding author. Tel.: +91 3222 281660; fax: +91 3222 255303.
*E-mail address:* anisarfat@yahoo.co.in (A. Anis).

0378-7753/$ – see front matter © 2007 Elsevier B.V. All rights reserved.
doi:10.1016/j.jpowsour.2007.12.041

cell performance. Consequently, a major research objective is to immobilize the HPAs in the polymer matrix and maintain its high proton conductivity. It is interesting to note that some inorganic–organic membranes, in which HPAs were well dispersed into hydrophilic polymer matrix, have been promising for polymer electrolyte membrane fuel cells (PEMFCs) and DMFC applications [17–24]. When HPAs were embedded in hydrophilic polymer matrix, they were expected to endow the composite membranes with their high proton conductivity, while retaining the desirable mechanical properties of the polymer membranes.

Poly(vinyl alcohol) (PVA) appears to be very attractive material as polymer matrix for preparing proton exchange membrane (PEM) because this polymer can function as an excellent methanol barrier [25]. PVA also has both very good mechanical properties and chemical stability, which are adequate for preparing PEMs [26]. Although PVA itself does not have fixed charges, several organic groups like hydroxyl, amine, carboxylate, sulfonate, and quaternary ammonium can be incorporated to impart hydrophilicity and/or ionic group [27,28]. Several crosslinking methods have been published for different use, since as a rule, all multifunctional compounds capable of reacting with hydroxyl groups can be used to obtain three-dimensional networks in PVA [29]. In our previous study [30–32], we reported the preparation of crosslinked membranes employing PVA as a polymer matrix, phosphomolybdic acid (PMA) to impart protonic conductivity and glutaraldehyde (GA) as a crosslinking agent. Kang et al. reported the preparation of PVA-based (i.e. PVA/poly(styrene sulfonic acid-co-maleic acid), PSSA-MA) PEM [33,34], using glutaraldehyde as a crosslinking agent. The proton conductivities and methanol permeability of the membranes were in the range of $10^{-2}$ S cm$^{-1}$ and $10^{-8}$–$10^{-6}$ cm$^2$ s$^{-1}$, respectively, depending on the blend conditions.

This paper reports the preparation of inorganic–organic composite membranes, with HPA immobilized in the polymer matrix. An ionic group containing PVA copolymer namely poly(vinyl alcohol-co-vinyl acetate-co-itaconic acid) has been used as a polymer matrix and PMA as the inorganic dopant. The composite membranes prepared were characterized by different characterization techniques.

## 2. Experimental

### 2.1. Materials and membrane preparation

Poly(vinyl alcohol-co-vinyl acetate-co-itaconic acid) (degree of hydrolysis approx. 97 mol%) was obtained from Aldrich; glutaraldehyde (25% content in water) was obtained from s.d. fine-Chemicals Ltd. (Mumbai, India) and PMA was obtained from Sisco Research Laboratories Pvt. Ltd. (Mumbai, India). Stock solution of the glutaraldehyde crosslinking reagent (CLR) was prepared by further diluting the obtained glutaraldehyde solution to 5% content in water. To prepare 5% (w/v) PVACO solution, PVACO was dissolved in water at 80 °C with continuous stirring. To 20 g of 5 wt.% PVACO solution, different amount of PMA was added and the resulting mixture was stirred until a homogeneous solution was obtained. To this solution desired amount of the glutaraldehyde crosslinking reagent was added and the solution was further stirred for few minutes. After that, the homogeneous solution was poured into Petri dish and allowed to dry at room temperature for 48 h. The membranes obtained were $100 \pm 10$ μm in thickness.

### 2.2. Infrared spectroscopy

Attenuated total reflection (ATR)-FTIR spectra in the range of 4000–600 cm$^{-1}$ of the composite polymer electrolyte membranes were obtained with FTIR Spectroscope (NEXUS-870, Thermo Nicolet Corporation) running Omnic software, and a uniform resolution of 2 cm$^{-1}$ was maintained in all cases.

### 2.3. Water uptake

Water uptake of the composite membranes was determined by measuring the change in the weight before and after hydration. The membrane was equilibrated in deionized water for 24 h at 25 °C, and the surface attached water on the membrane was removed carefully by placing both the surfaces of the membranes gently over a filter paper. The weight of the wetted membrane was determined quickly using an analytical balance with a sensitivity of 0.1 mg. Water uptake was calculated by using the following equation:

$$\text{Water uptake} = \frac{M_w - M_d}{M_d} \quad (1)$$

where $M_w$ and $M_d$ is the weight of the swollen polymer and dry polymer in grams, respectively.

### 2.4. Dopant loss

Titration method was used to determine the dopant loss from the membranes due to bleeding out of the HPAs upon hydration. Each composite membrane was soaked in 50 ml of deionized water for 24 h at ambient temperature. Then, 10 ml of the solution was titrated with 0.01N NaOH. The dopant loss was calculated by using the following equation:

$$\text{DL} = \frac{A \times 0.01 \times 5}{m} \quad (2)$$

where DL is the dopant loss (meq. g$^{-1}$), $A$ the NaOH used to neutralize the resulting aqueous solution after equilibration (ml), 0.01 the normality of the NaOH, 5 the factor corresponding to the ratio of the amount of water taken to equilibrate the polymer to the amount used for titration, and $m$ the sample mass (g).

### 2.5. Impedance spectroscopy

Conductivity measurements were made at room temperature after equilibrating the membrane in deionized water for 24 h. The membrane was sandwiched between stainless steel electrodes; ac impedance spectra of the membranes were obtained by using Agilent 4294A Precision Impedance Analyzer under an oscillation potential of 10 mV from 40 Hz to 10 MHz. The

conductivity was calculated from the bulk resistance obtained from the high frequency intercept of the imaginary component of impedance with the real axis. The conductivity of the membrane is determined by $\sigma = (1/R_b)(L/A)$, where $R_b$, $L$ and $A$ represent bulk resistance, membrane thickness and area of the electrode, respectively.

### 2.6. Methanol permeability measurement

Diffusion coefficient measurements were performed using an in house built diffusion cell having two compartments, which were separated by the membrane situated horizontally. Prior to measurements, the membranes were equilibrated in aqueous methanol solution 50% v/v for 24 h and the experiments were carried out at room temperature. The methanol concentration of the receptor compartment was estimated using a differential refractometer (Photal OTSUKA Electronics, DRM-1021); the differential refractometer is highly sensitive to the presence of methanol. The change in refractive index of the diffusion samples were averaged over 52 scans in the differential refractometer to determine the change in refractive index.

### 2.7. Thermo gravimetric analysis

Thermal stability of the pristine polymer and the composite membranes was carried out by using NETZSCH TG 209 F1 at a heating rate of 10 °C min$^{-1}$, with nitrogen flushed at 100 ml min$^{-1}$.

### 2.8. Mechanical properties

The tensile strength of the composite membranes was carried out using Hounsfield H10KS tensile testing machine at a crosshead speed of 12.5 mm min$^{-1}$, temperature 27 °C and 75% relative humidity. The gauge dimension of the dog bone shaped test samples was 5 mm × 50 mm. For each sample, three specimens were tested and average value of tensile strength and percent elongation at break is reported.

### 2.9. Atomic force microscopy

Atomic force microscopy was performed using a Digital Instruments 3000 AFM, controlled by the Nanoscope IIIa scanning probe microscope controller with a Nanoprobe Tapping (TESP) SPM tip from Digital Instruments, CA. The tapping tip is mounted on 125 μm long, single beam cantilevers, with resonant frequencies in the range of 330–399 kHz and corresponding spring constants of 20–100 N m$^{-1}$.

### 2.10. Transmission electron microscopy

To obtain a better estimate of the particle size of the dispersed PMA in the composite PEM they were studied by TEM. Reichert Ultracut E Cryo-Ultramicrotome was used for ultra-microtomy to obtain thin sections of the samples. The ultra-microtomed sections were placed on copper grids and studied using a JEOL 1400 transmission electron microscope at an accelerating voltage of 100 kV. The JEOL 1400 also con-

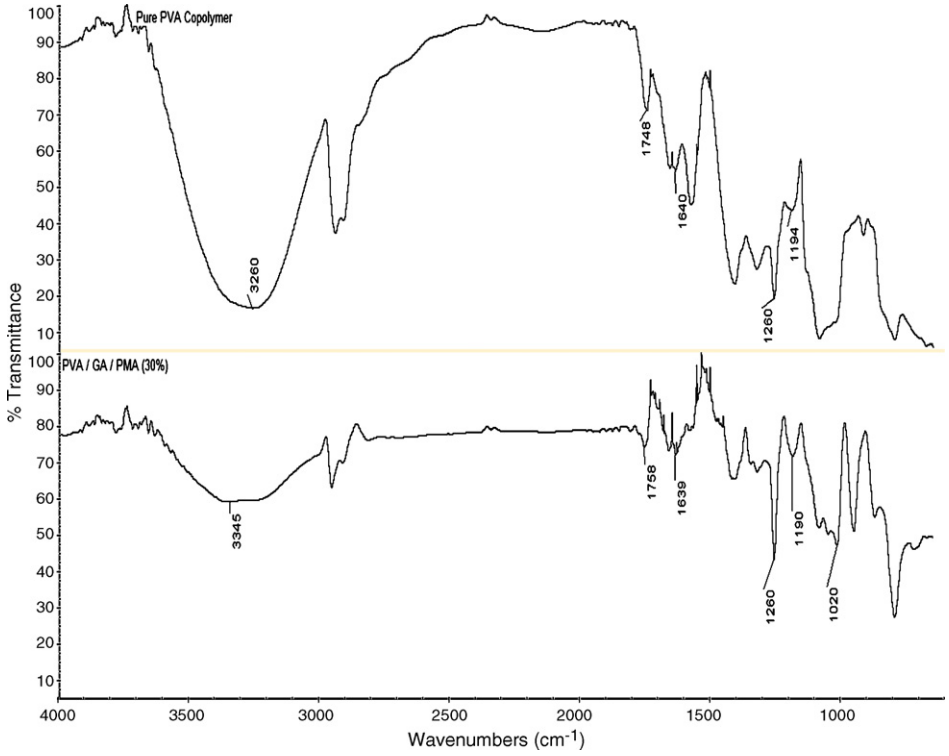


Fig. 1. FTIR spectra of pure PVACO and PVACO/PMA composite chemically crosslinked with glutaraldehyde.

tains a Gatan CCD, which facilitates the acquisition of digital images.

## 3. Results and discussion

### 3.1. FTIR-ATR spectroscopy

The IR spectrum of pure PVA copolymer membrane (Fig. 1) shows the major peaks associated with the PVA copolymer. The spectrum shows a broad C–H alkyl stretching band (2850–3000 $cm^{-1}$) and typical strong hydroxyl bands for hydrogen-bonded alcohol (3200–3570 $cm^{-1}$). Intramolecular and intermolecular hydrogen bonding are expected to occur among PVA chains due to high hydrophilic forces. The peaks at 1640 and 1748 $cm^{-1}$ is due to C=O stretching of saturated aliphatic esters (acetate) and carboxylic acid (itaconic acid) groups, respectively. The broad absorption band from 1000–1320 $cm^{-1}$ can be attributed to the (C–O) stretching of alcohol, ester and carboxylic acid groups of the PVA copolymer.

The IR spectrum of the glutaraldehyde crosslinked PVACO/PMA composite membrane (Fig. 1) shows a decrease in the intensity of the O–H stretching vibration peak (3200–3500 $cm^{-1}$) due to the crosslinking reaction of glutaraldehyde with the hydroxyl groups of PVACO. The weak peak of the C=O band (1640 $cm^{-1}$) indicates that the aldehyde groups of glutaraldehyde have completely reacted with O–H groups of the PVACO chain in the presence of PMA, which acts as a catalyst for the PVACO–glutaraldehyde crosslinking reaction. The increase in intensity of the C–O stretching peaks at 1260, 1190, 1020 $cm^{-1}$ and the frequency shift of the peak at 1194–1190 $cm^{-1}$ further confirms to the formation of ether (C–O) and the acetal ring (C–O–C) linkages due to the crosslinking reaction of PVACO with glutaraldehyde.

The IR spectra of the PVACO/PMA composite membranes with same weight percent of PMA content but with different amount of glutaraldehyde crosslinking reagent is shown in Fig. 2. When the volume of the glutaraldehyde crosslinking reagent was increased, a decrease in intensity of the O–H stretching vibration peak and increase in intensity of the peaks associated with the formation of ether (C–O) and the acetal ring (C–O–C) linkages was observed. Therefore, it is safe to assume that glutaraldehyde has acted as chemical crosslinker among PVA copolymer chains.

The IR spectra of pure PMA and the influence of PMA addition on the skeletal modes in the polymer composites are shown in Fig. 3. The IR spectrum of pure PMA shows the typical features of Keggin anions. According to the assignments of Rocchiccioli-Deltcheff et al. [35], the four absorption bands at 1064, 961, 868, 780 $cm^{-1}$ are assigned to the $\nu$(P–O), $\nu$(Mo–$O_t$) ($O_t$ refers to the terminal oxygen), $\nu$(Mo–$O_c$–Mo) ($O_c$ refers to the corner oxygen) and $\nu$(Mo–$O_e$–Mo) ($O_e$ refers to the edge oxygen), respectively. All these characteristic bands of PMA are also present in the spectra of the composites, indicating the preservation of Keggin ions geometry inside the polymer composites. The most pronounced change, which appears in spectra of composites, is the shift of the $\nu$(P–O) stretching mode peak towards higher wave numbers. The observed effect is stronger for systems with lower acid concentration and the shift increases with increase in the PMA concentration. Similar behaviour was observed for many HPA containing systems,

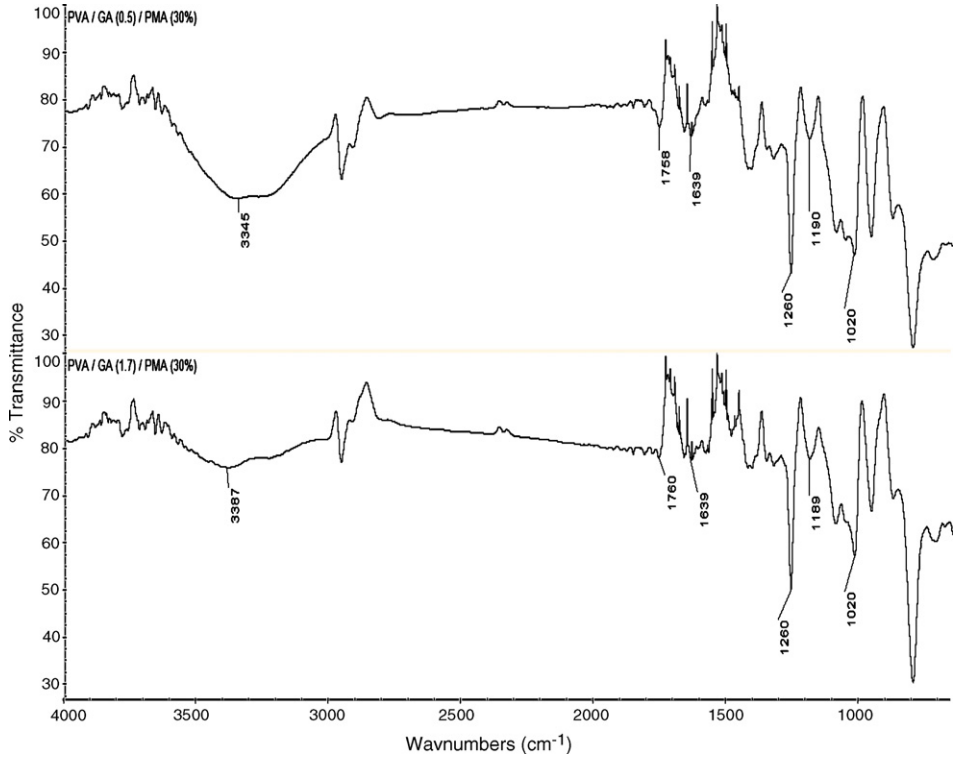


Fig. 2. FTIR spectra of crosslinked PVACO/PMA composites with different crosslinking reagent (CRL).

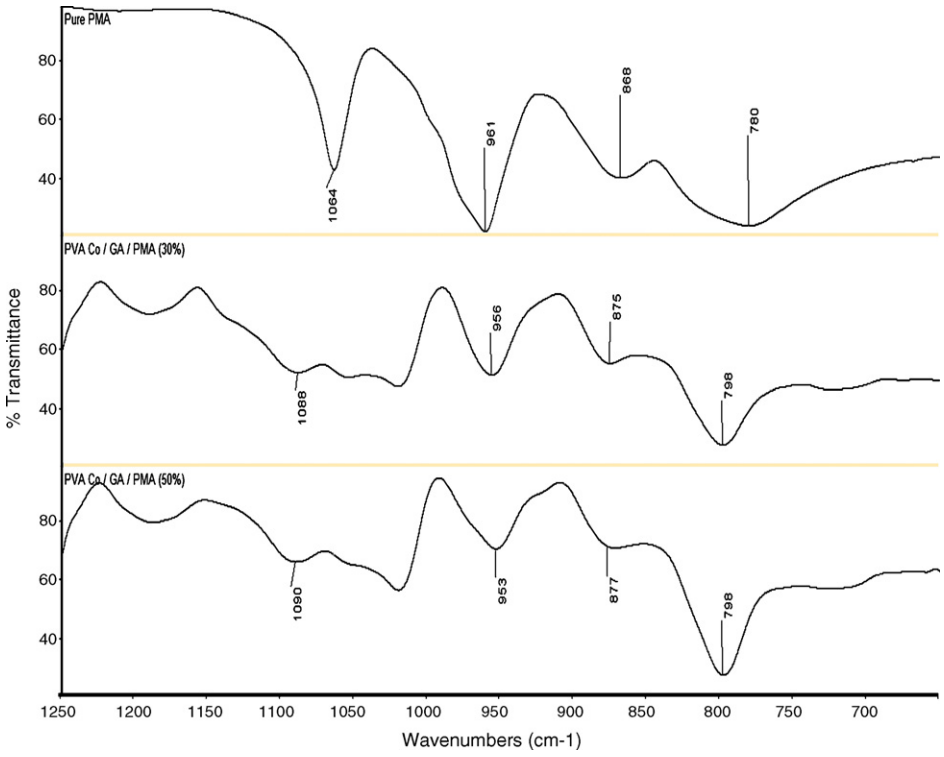


Fig. 3. FTIR spectra of pure PMA and the PVACO/PMA composites with different PMA content.

e.g. for $SiO_2$/silicotungstic acid composites [36] and is due to the increase in the distance between the anions and hence the weakening of dipolar interactions. An upward shift is also observed for the $\nu$(Mo–$O_c$–Mo) and $\nu$(Mo–$O_e$–Mo) stretching vibrations, whereas bands ascribed to the stretching vibration $\nu$(Mo–$O_t$) moves to lower frequencies with increase in PMA content of the composite membranes. These frequency shifts clearly demonstrate that there is specific interaction between Keggin structure of PMA molecules and the PVA copolymer, which is probably both the terminal oxygen and the bridging oxygen interact with the hydroxyl and carboxylic acid groups of the copolymer.

### 3.2. Water uptake

The water uptake of the crosslinked pure PVACO and the PVACO/PMA composite membranes are shown in Fig. 4. The glutaraldehyde crosslinked membranes of pure PVACO with 0.5 ml CLR showed a water uptake of 4.8 g $g^{-1}$ of the dry polymer and even at this level of water content the crosslinked membrane reasonably retained its mechanical properties. A reduction of more than 60% in the water uptake of the membrane was observed by the incorporation of 10 wt.% of PMA in the membranes, when the PMA content of the membranes was increased to 30 wt.% a slight increase in the water uptake of the composite membranes was observed which is due to hydrophilic nature of the PMA. Further increase in the PMA content of the composite membranes (50 wt.%) leads to a decrease in water uptake of the membrane, this decrease in water uptake is due to the resistance offered by the crosslinked networks which restrict the swelling of the polymer networks. The crosslinked polymer networks very well control the hydrophilic character of the composite membranes by restricting the swelling of the polymer networks and hence their water uptake.

The water uptake of the crosslinked PVA copolymer membranes (without PMA) decreases with increase in CLR content of the membrane. A further decrease in water uptake is observed for the composite membrane by the incorporation of 30 wt.% PMA in the crosslinked composite membranes. The increase in CLR content of the PVACO/PMA composite membrane leads to decrease in water uptake of the composite membranes. The minimum water uptake of 1.03 g $g^{-1}$ of the composite was observed for the membrane with 30% PMA content and 1.7 ml of glutaraldehyde crosslinking reagent, this is substantially higher than

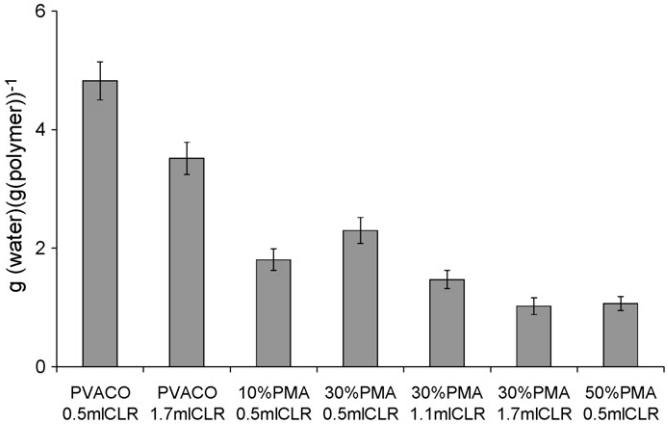


Fig. 4. Water uptake of pure PVA copolymer and the PVACO/PMA composites.

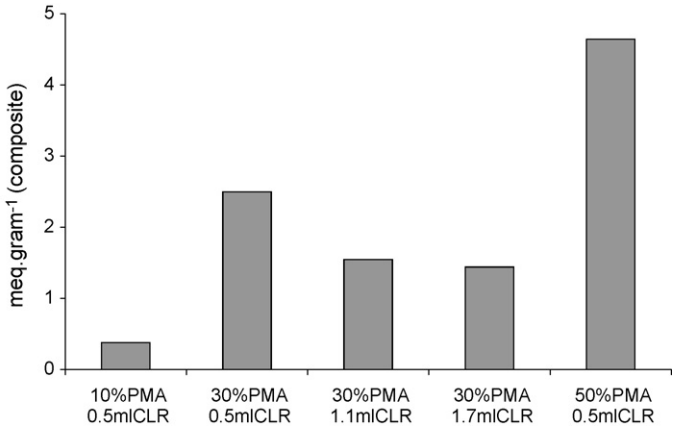


Fig. 5. Dopant loss from the PVACO/PMA composites.

that reported for Nafion 117 (0.27 g $g^{-1}$) under similar measurement conditions [37].

### 3.3. Dopant bleeding

The major problem associated with composite polymer electrolyte membranes is the bleeding out of dopant from the polymer matrix in fuel cell environment, which leads to depleted performance of the membrane with time. This phenomenon is investigated in the present study by determining the dopant loss from the PVA/PMA composite membranes by titration method. The dopant loss values of the composite membranes with different PMA and CLR content is shown in Fig. 5.

The dopant loss increases sharply with increase in PMA content of the membrane. Hence increase in percent content of the component which imparts the proton conductivity to the composite membrane is not always desirable. In order to further enhance the immobilization of the PMA in the composite membranes the CLR content of the membranes was increased. It was observed that with increase in CLR content of the composite membranes the dopant loss from the membrane decreased.

### 3.4. Conductivity

The room temperature conductivity of the crosslinked pure PVA copolymer membranes as well as for the composite membranes with different PMA and CLR content is shown in Fig. 6. The carboxylic acid group provides conductivity in the pristine PVA copolymer membrane. The conductivity of the pristine membrane decreases with increase in crosslink density of the membrane, which can be, attributed to the decrease in water uptake of the membrane with increase in crosslink density of the membranes. This result points to the fact that conductivity is a strong function of water content of membranes with pendent ionic groups.

The decrease in conductivity on incorporation of PMA in the pure PVACO is due to decrease in water uptake of the composite membranes with 10 and 30 wt.% PMA content, further increase in PMA content of the composite membranes to 50 wt.% leads to a substantial increase in the conducting behaviour of the composite membranes.

The conductivity of the composite membranes increases with increase in crosslink density of the membranes together with continuous decrease in water uptake of the membrane. This method of preparing composite membrane is very useful because it very precisely helps us to control the water uptake of the hydrophilic polymer-based PEM which in turn helps in improving their mechanical property as well as conductivity of the composite membranes at the same time, which is highly desirable. The incorporation of PMA helps to enhance the conductivity of ionic polymer-based PEMs even at low water content and further helps in retaining this conductivity at higher temperatures.

Since DMFC application requires membrane quality that attains high proton conductivity and low methanol permeability, the membrane selectivity can be evaluated using the following expression:

$$\phi = \frac{\sigma}{D} \tag{3}$$

where $\phi$ is a parameter that evaluates the selectivity of the membrane for DMFC application in terms of the ratio of the proton conductivity ($\sigma$) to the methanol permeability ($D$). The selectivity values for the prepared PVACO/PMA composites and Nafion 117 have been reported in Table 1.

The temperature dependence behaviour of the conductivity in polymer electrolytes has often been taken as indicative of a particular type of conduction mechanism. The dependence of proton conductivity on temperature follows two different types of equations according to two different kinds of proton-transport mechanism. Arrhenius law Eq. (4) can be used to explain the proton hopping mechanism, while the segmental motion mech-

Table 1
Selectivity value for the PVACO composites and Nafion 117

| PMA content (wt.%) | CLR content (ml) | Conductivity $\times 10^{-3}$ (S $cm^{-1}$) | Methanol permeability $\times 10^{-6}$ ($cm^2$ $s^{-1}$) | Selectivity $\phi \times 10^3$ (S $cm^{-3}$ s) |
|---|---|---|---|---|
| 0 | 0.5 | 1.66 | 3.71 | 0.45 |
| 0 | 1.7 | 0.55 | 2.16 | 0.25 |
| 10 | 0.5 | 0.52 | 1.58 | 0.32 |
| 30 | 0.5 | 0.71 | 1.79 | 0.39 |
| 30 | 1.1 | 1.45 | 1.69 | 0.86 |
| 30 | 1.7 | 2.05 | 1.54 | 1.33 |
| 50 | 0.5 | 2.68 | 3.92 | 0.68 |
| Nafion | | 62.0 | 6.50 | 9.54 |

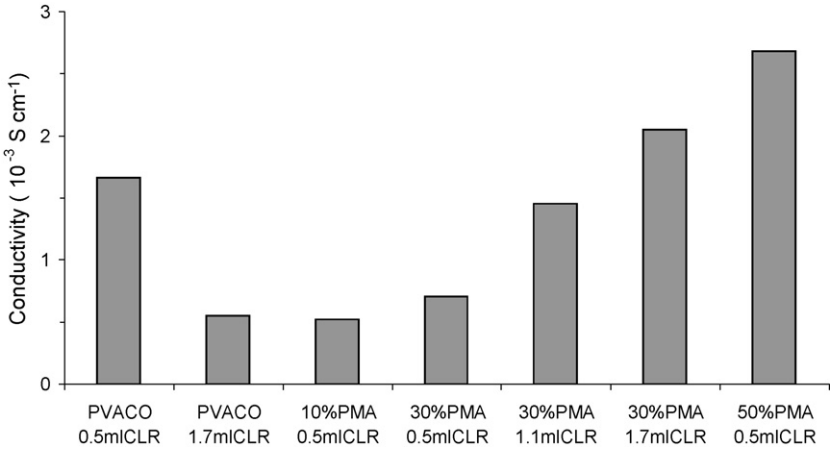


Fig. 6. Conductivity of pure PVA copolymer and the PVACO-PMA composites.

anism fits VTF Eq. (5):

$$\sigma = \sigma_0 \exp\left(-\frac{E_a}{RT}\right) \quad (4)$$

$$\sigma = A \exp\left(-\frac{B}{R(T - T_0)}\right) \quad (5)$$

$\sigma_0$ is the pre-exponential factor, $E_a$ the apparent activation energy, $R$ the Boltzmann constant and $T$ the temperature of polymer electrolytes. $A$, $B$ and $T_0$ are three parameters. $R$ and $T$ are the same as that of Arrhenius equation.

Fig. 7 shows the ionic conductivity of the crosslinked pure PVACO and the PVACO-PMA composite membranes against the reciprocal absolute temperature, the linear relationship confirms that the variation in conductivity with temperature follows an Arrhenius relationship. For the pure PVA copolymer membranes, the activation energy was found to increase from 0.16 to 0.23 eV with increase in CLR content of the membrane from 0.5 to 1.7 ml.

For the composite membranes with different wt.% PMA content, the activation energy was found to decrease markedly as the acid content of the membranes increased with a value of 0.28 eV for 10 wt.% PMA content and 0.16 eV for 50 wt.% PMA content of the membranes. A similar behaviour was also observed for the composite membranes with 30 wt.% PMA content and dif-

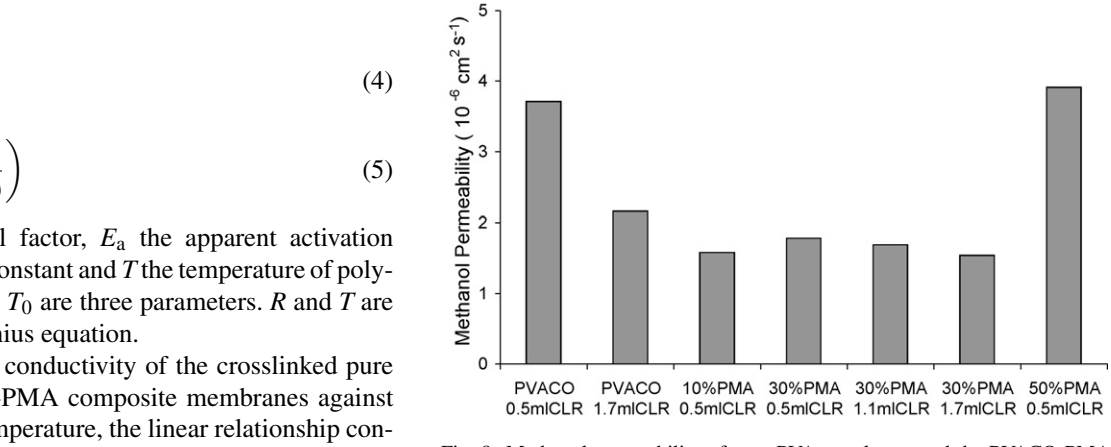


Fig. 8. Methanol permeability of pure PVA copolymer and the PVACO-PMA composites.

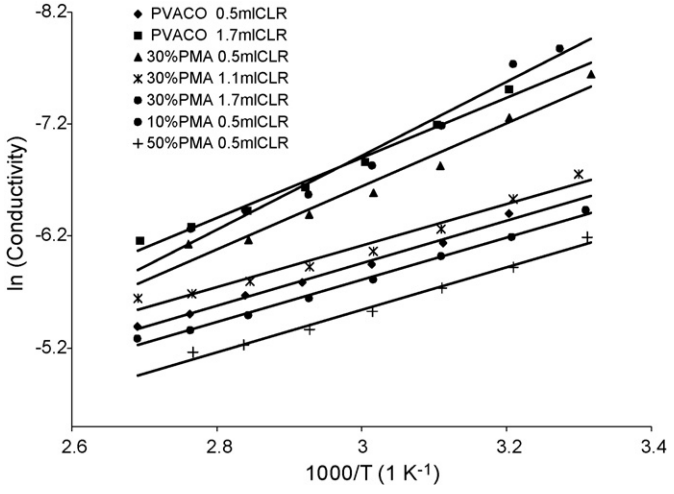


Fig. 7. Arrhenius plots for pure PVA copolymer and the PVACO-PMA composites.

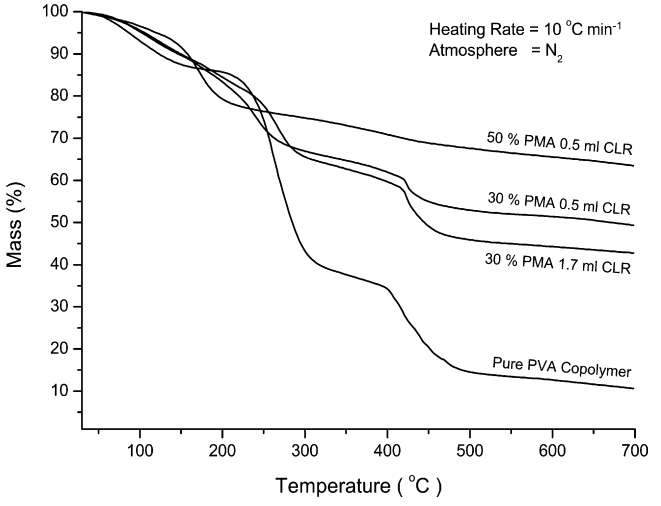


Fig. 9. TGA thermograms of pure PVA copolymer and the PVACO/PMA composites.

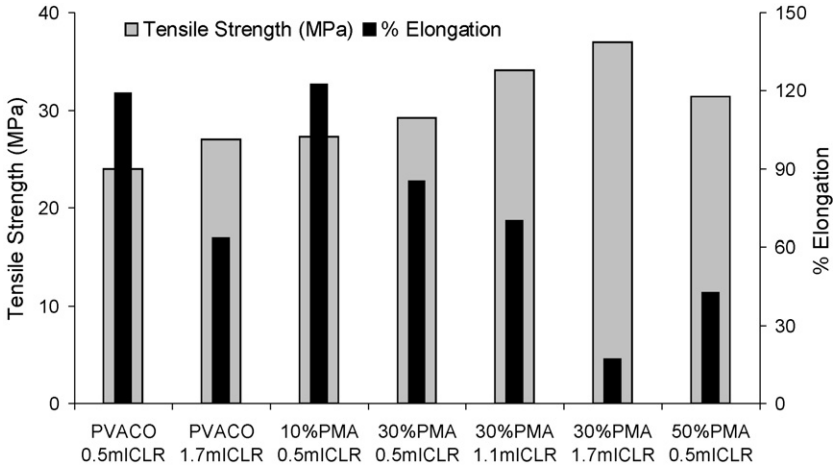


Fig. 10. Mechanical properties of pure PVA copolymer and the PVACO/PMA composites.

ferent CLR content, the activation energy was found to decrease from 0.24 to 0.16 eV with increase in CLR from 0.5 to 1.7 ml. Such behaviour is classically observed with glasses for which the results are interpreted by the weak electrolyte model [38].

The Arrhenius behaviour observed in the present work shows that the conductivity is controlled by a hopping mechanism, therefore it can be suggested that the conductivity is governed by a hopping mechanism in the temperature range of the study. However, the values of the activation energy, much higher than those for pure acids suggest that the mechanism of the conduction is different from that occurring in the pure acids.

### 3.5. Methanol permeability

The methanol permeability of the crosslinked pure PVA copolymer membranes as well as for the composite membranes with different PMA and CLR content is shown in Fig. 8. The pristine membrane showed high methanol permeability compared to the composite membranes with different PMA content due to the high water uptake of this particular membrane. A reduction of almost 50% was observed in the methanol permeability of the composite membrane by the incorporation of 10 wt.% of PMA in the membranes, when the PMA content of the membranes was further increased to 30 wt.% a slight increase in the methanol permeability of the composite membranes was observed. With further increase in the PMA content of the composite membranes to 50 wt.% a sharp increase in methanol permeability of the membrane was observed, this trend in increase in methanol permeability of the membranes is similar to the dopant loss behaviour of these composite membranes. As the dopant loss from the membrane increases the membrane becomes more and more permeable to methanol, hence effective immobilization

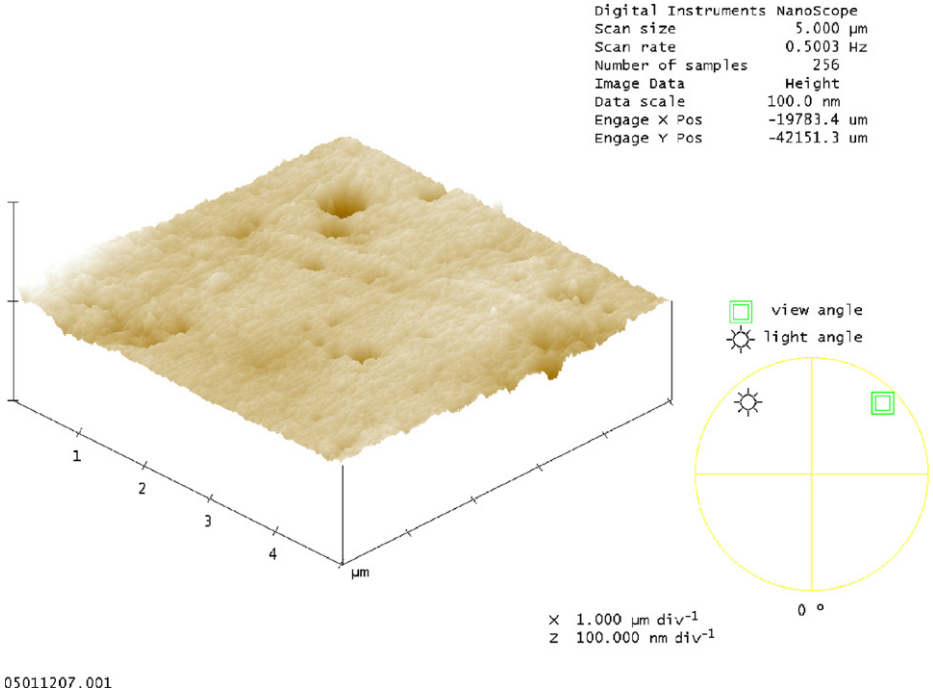


Fig. 11. Tapping mode AFM images (3D) of pure uncrosslinked PVA copolymer.

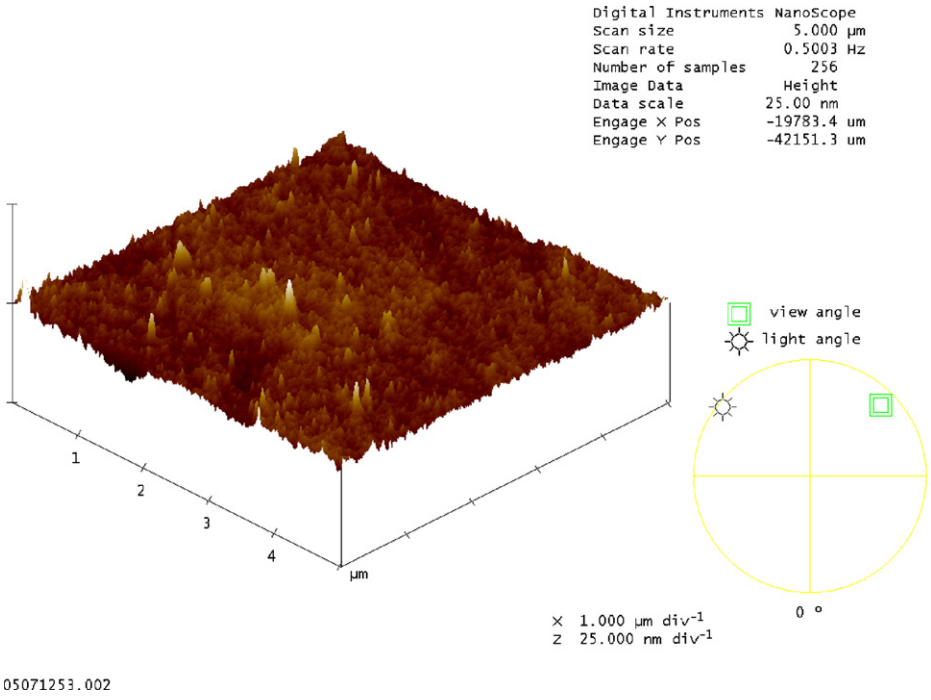


Fig. 12. Tapping mode AFM images (3D) of pure PVA copolymer (1.7 ml CLR).

of the dopant in the polymer matrix by optimizing the crosslink density can be an effective strategy for minimizing the methanol permeability.

The methanol permeability of the PVA copolymer membrane (without PMA) decreases with increase in the crosslink density of the membrane. A further decrease in methanol permeability is observed for the composite membrane with 30% PMA content which further decreases with increase in crosslink density of the membranes. The minimum methanol permeability of $1.54 \times 10^{-6}$ cm$^2$ s$^{-1}$ was observed for the composite membranes with 30% PMA content and 1.7 ml of glutaraldehyde crosslinking reagent.

### 3.6. Thermo gravimetric analysis

The thermal stability of the PVACO-PMA composite membranes with different PMA content and crosslink density was

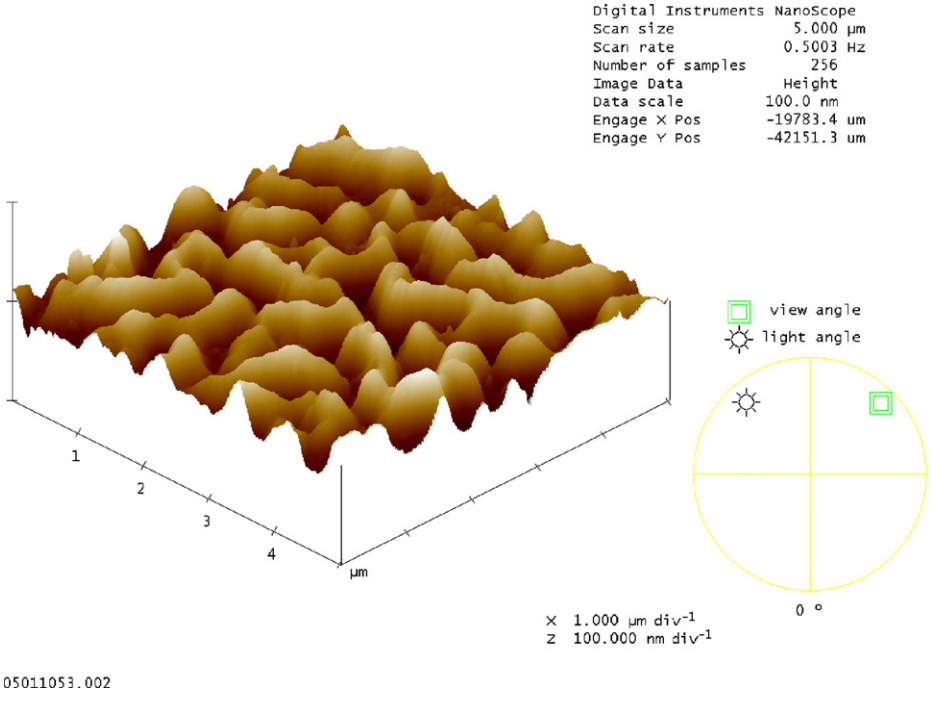


Fig. 13. Tapping mode AFM images (3D) of PVACO-PMA composite (30% PMA/0.5 ml CLR).

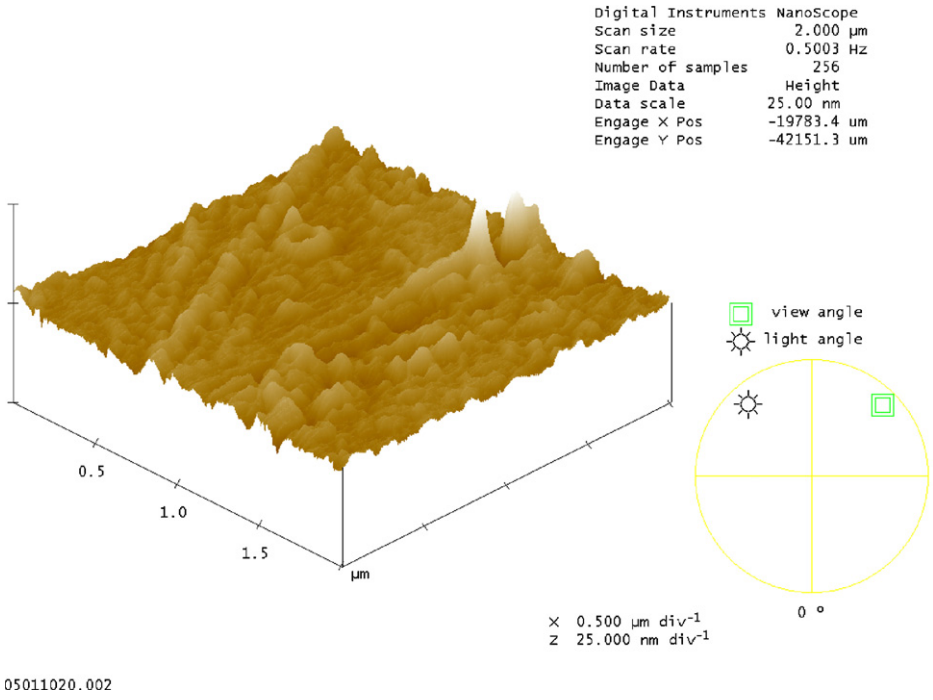


Fig. 14. Tapping mode AFM images (3D) of PVACO-PMA composite (50% PMA/0.5 ml CLR).

investigated by thermo gravimetric analysis. Fig. 9 shows TGA thermograms of pristine PVA copolymer and the representative composite membranes in $N_2$ atmosphere. The pristine PVA remains stable up to 230 °C. It can be seen that three consecutive weight loss steps were observed for the PVA/PMA composite membranes. Each weight loss step is responsible for a thermal solvation, thermal degradation of the crosslinks (ester and ether linkages) and finally a thermal oxidation of the polymer chain, respectively. The PVA/PMA composite membranes show enhanced thermal stability and the composite membrane shows a loss of about 15–20 wt.% of their weight at around 180 °C. It corresponds to weight loss of absorbed water, structural water associated with PMA and water as by-product by further esterification in the PVA/PMA membranes. The second weight loss of 10–15 wt.% at around 250–450 °C is due to the thermal degradation of the ether and ester crosslinking linkages. The third

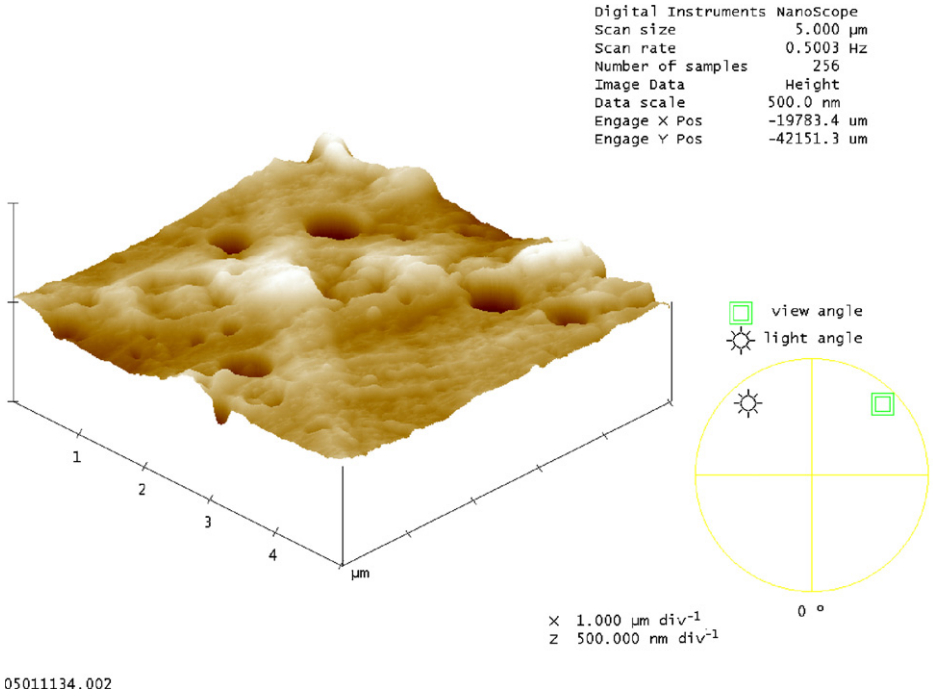


Fig. 15. Tapping mode AFM images (3D) of PVACO-PMA composite (30% PMA/1.7 ml CLR).

weight loss is due to degradation of the polymer backbone and/or reaction with air, which starts at around 600 °C.

### 3.7. Mechanical properties

The tensile strength and percent elongation at break of the crosslinked pure PVA copolymer membranes as well as for the composite membranes with different PMA and CLR content is shown in Fig. 10. Tensile strength of 18 MPa and percent elongation of 430% was observed for pristine PVACO membrane (uncrosslinked), when the PVACO membrane is crosslinked with glutaraldehyde the tensile strength for the pure crosslinked membranes increases with increase in CLR content whereas a reverse trend is observed for the percent elongation at break.

The tensile strength for the composite membranes increases slightly with the incorporation of PMA and is further augmented with the increase in PMA content of the membrane. The percent elongation at break for the composite membranes with different wt.% PMA content initially increases with the incorporation of PMA in the pristine PVA copolymer membrane and then decreases with further increase in PMA content. This decrease in percent elongation can be due to the esterification of the hydroxyl groups of PVA and hence resulting in reduction in the extent of hydrogen bonding between the hydroxyl groups of PVACO.

The tensile strength of the composite membranes with different CLR content increases with increase in CLR whereas the percent elongation at break decreases with increase in crosslink density of the membrane. From the results it can be observed that the crosslinked membranes exhibit higher tensile strength than the pristine PVACO. This enhancement in tensile strength and decrease in percent elongation is due to the formation of crosslinked networks hence restricted mobility of the polymer chains.

### 3.8. Atomic force microscopy

The tapping mode 3D AFM images of the pure PVA copolymer (uncrosslinked and crosslinked) and crosslinked PVACO-PMA composite membrane surfaces are shown in Figs. 11–15. Quantitatively, the differences in the morphology can be expressed in terms of various roughness parameters such as the mean roughness $R_a$, the root mean square (rms) of vertical data $R_q$, and the maximum height $R_{max}$. Here, the mean roughness is the mean value of surface relative to the center plane, the plane for which the volume enclosed by the image above and below this plane are equal; $R_{max}$ the height difference between the highest and lowest points on the surface relative to the mean plane and $R_q$ is the standard deviation of the $Z$ values within the given area. The roughness parameters were calculated for all membrane surfaces and the results are summarized in Table 2.

Table 2
Roughness parameters for different membrane surfaces

| Membrane | $R_a$ (nm) | $R_{max}$ (nm) | $R_q$ (nm) |
|---|---|---|---|
| Pure PVACO | 3.06 | 108.30 | 5.467 |
| PVACO 1.7 ml CLR | 0.73 | 15.45 | 0.97 |
| 30% PMA 0.5 ml CLR | 12.16 | 85.11 | 14.31 |
| 50% PMA 0.5 ml CLR | 1.11 | 128.98 | 2.63 |
| 30% PMA 1.7 ml CLR | 25.77 | 326.67 | 37.65 |

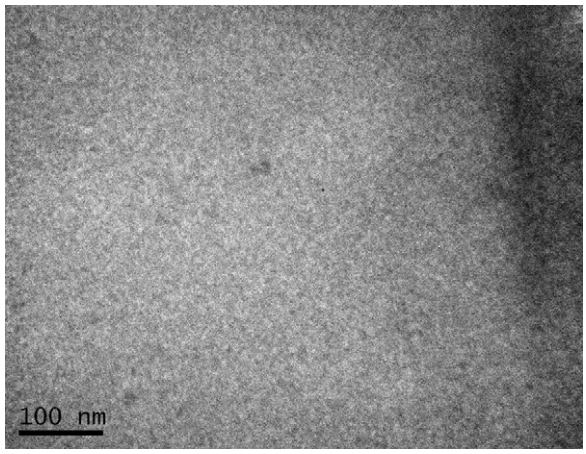


Fig. 16. TEM image of PVACO-PMA composite (30% PMA/0.5 ml CLR).

The AFM images of pure PVACO membranes show a significant change in surface morphology on crosslinking. The AFM images of uncrosslinked PVA copolymer membrane shows a porous morphology (about 0.5 μm in diameter) and the mean roughness of 3.10 nm for the surface topography of the membrane, whereas the crosslinked PVA copolymer membrane with 1.7 ml CLR shows a homogeneous, non-porous surface morphology and also a much smoother surface topography, mean roughness of 0.73 nm. The composite membrane with 30 wt.% PMA content (Fig. 13) shows a homogeneous and non-porous morphology and retains these properties even with further increase of PMA content of the composite membranes to 50 wt.% (Fig. 14). The mean roughness for the surface topography of the membrane decreases from 12.16 to 1.11 nm with increase in PMA content of the composite membranes from 30 to 50 wt.%. This shows that there is a good compatibility between the HPA and the PVA copolymer matrix. When the crosslink density of the composite membrane with 30 wt.% PMA content is increased from 0.5 to 1.7 ml CLR (Fig. 15) then the membrane developed a porous morphology (about 0.5 μm in diameter) and the mean roughness of the surface of the membrane increased from 12.16 to 25.77 nm.

### 3.9. Transmission electron microscopy

The TEM image (Fig. 16) shows a homogeneous nano-phase separation at a scale of 10–20 nm, where the bright regions represent inorganic rich phases, and dark region, the organic rich phase [39]. Similar binary phase nano-scale separation have also been reported by Kim et al. [40] for organic–inorganic hybrid membranes containing phosphotungstic acid as proton source for application in intermediate temperature PEMFC.

## 4. Conclusion

Novel organic–inorganic crosslinked composite polymer electrolyte membranes were developed by successfully immo-

bilizing PMA in the PVACO matrix. FTIR spectroscopy was used to characterize the occurrence of the chemical crosslinking reaction. Chemical crosslinking of the polymer matrix helped in controlling the water uptake of the composite membranes and also in retention of the PMA in the polymer matrix. The proton conductivity of the composite membranes was of the order of $10^{-3}$ S cm$^{-1}$ which is an order lower than the commercially available membranes. The methanol permeability was of the order of $10^{-6}$ cm$^2$ s$^{-1}$ and was always lower compared to the Nafion membrane measured under similar conditions. The composite PEM were found to be thermally more stable than the pristine polymer. The topographical feature of the membrane surface was successfully characterized by atomic force microscopy in tapping mode (TM-AFM). The TEM studies showed a homogeneous nano-phase dispersion of the PMA particles in the PVACO polymer matrix. The PVA copolymer used is biodegradable, non-hazardous and environmentally benign.

The PVACO/PMA composite with 30 wt.% PMA and 1.7 ml CLR content is found to the best among all the PEMs prepared. In particular this composite membrane shows the highest proton conductivity (except 50 wt.% PMA membrane) together with lowest water uptake, lowest dopant loss, lowest methanol permeability, highest tensile strength and enhanced thermal stability among all the PEMs prepared. The presence of PMA in the composites makes it a better candidate in retaining the proton conductivity at higher temperatures. Hence it is safe to conclude that the PVACO/PMA membrane with 30 wt.% PMA and 1.7 ml CLR is the better candidate over the crosslinked pure PVACO membranes as well as the other PVACO/PMA composite membranes. Comparatively very low cost of PVACO and PMA used for the preparation of these PEMs to that of Nafion make these composites an interesting and potential alternative proton conducting PEMs. These composite membranes will be considerably less durable as compared to Nafion due to the absence of fluorine chemistry but might be preferable in certain cases owing to very low cost of production and environment friendliness of these composite PEMs.

## Acknowledgements

The authors wish to thank the Australia–India Council, Canberra for providing partial funding to enable visiting fellow Mr. Arfat Anis to work at University of New South Wales, Sydney, Australia.

## References

[1] Y. Tsai, S. Li, J. Chen, Langmuir 21 (2005) 3653–3658.
[2] R. Mukundan, E. Brosha, F. Garzon, Solid State Ionics 175 (2004) 497–501.
[3] M. Alvaro, A. Corma, D. Das, V. Fornes, H. Garcia, J. Catal. 231 (2005) 48–55.
[4] B.J. Landi, R.P. Raffaelle, M.J. Heben, J.L. Alleman, W. VanDerveer, T. Gennett, Mater. Sci. Eng. B 115 (2005) 359–362.
[5] A. Yamauchi, K. Togami, A.M. Chaudry, A.M. El Sayed, J. Membr. Sci. 249 (2005) 119–126.
[6] K. Miyatake, M. Watanabe, Electrochemistry 73 (2005) 12–19.
[7] W.H.J. Hogarth, J.C.D. Costa, G.Q. Lu, J. Power Sources 142 (2005) 223–237.
[8] B. Mecheri, A. D'Epifanio, M.L.D. Vona, E. Traversa, S. Licoccia, M. Miyayama, J. Electrochem. Soc. 153 (2006) A463–A467.
[9] C. Yang, S. Srinivasan, A.S. Aricò, P. Cretì, V. Baglio, V. Antonucci, Electrochem. Solid State Lett. 4 (2001) A31–A34.
[10] G.M. Haugen, F. Meng, N.V. Aieta, J.L. Horan, M.C. Kuo, M.H. Frey, S.J. Hamrock, A.M. Herring, Electrochem. Solid State Lett. 10 (2007) B51–B55.
[11] V. Ramani, H.R. Kunz, J.M. Fenton, J. Membr. Sci. 266 (2005) 110–114.
[12] V. Ramani, H.R. Kunz, J.M. Fenton, J. Power Sources 152 (2005) 182–188.
[13] V. Ramani, H.R. Kunz, J.M. Fenton, Electrochim. Acta 50 (2005) 1181–1187.
[14] F.A. Cotton, G. Wilkinson, C.A. Murillo, M. Bochmann, Advanced Inorganic Chemistry, John Wiley & Sons, 1999, pp. 926–933.
[15] H. Kim, M.S. Kang, D.H. Lee, J. Won, J. Kim, Y.S. Kang, J. Membr. Sci. 304 (2007) 60–64.
[16] A.M. Herring, Polym. Rev. 46 (2006) 245–296.
[17] O. Savadogo, J. Power Sources 127 (2004) 135–161.
[18] S.M.J. Zaidi, S.D. Mikhailenko, G.P. Robertson, M.D. Guiver, S. Kaliaguine, J. Membr. Sci. 173 (2000) 17–34.
[19] B. Bonnet, D.J. Jones, J. Rozière, L. Tchicaya, G. Alberti, M. Casciola, L. Massinelli, B. Bauer, A. Peraio, E. Ramunni, J. New Mater. Electrochem. Syst. 3 (2000) 87–92.
[20] S. Malhotra, R. Datta, J. Electrochem. Soc. 144 (1997) L23–L26.
[21] M.L. Ponce, L. Prado, B. Ruffmann, K. Richau, R. Mohr, S.P. Nunes, J. Membr. Sci. 217 (2003) 5–15.
[22] Y.S. Kim, F. Wang, M. Hickner, T.A. Zawodzinski, J.E. McGrath, J. Membr. Sci. 212 (2003) 263–282.
[23] B. Tazi, O. Savadogo, Electrochim. Acta 45 (2000) 4329–4339.
[24] L. Li, Y.X. Wang, Chin. J. Chem. Eng. 100 (2002) 614–617.
[25] S. Bryan, B.S. Pivovar, Y. Wang, E.L. Cussler, J. Membr. Sci. 154 (1999) 155–162.
[26] S.Y. Kim, H.S. Shin, Y.M. Lee, C.N. Jeong, J. Appl. Polym. Sci. 73 (1999) 1675–1683.
[27] J.F. Blanco, Q.T. Nguyen, P. Schaetzel, J. Membr. Sci. 186 (2001) 267–279.
[28] H.B. Park, S.Y. Nam, J.W. Rhim, J.M. Lee, S.E. Kim, J.R. Kim, Y.M. Lee, J. Appl. Polym. Sci. 86 (2002) 2611–2617.
[29] M. Krumova, D. Lopez, R. Benavente, C. Mijangos, J.M. Perena, Polymer 41 (2000) 9265–9272.
[30] A. Anis, A.K. Banthia, Int. J. Plast. Technol. 9 (2005) 539–545.
[31] A. Anis, S. Mondal, A.K. Banthia, A.K. Thakur, Chin. J. Polym. Sci. 5 (2006) 449–456.
[32] A. Anis, A.K. Banthia, Mater. Manuf. Process. 22 (2007) 1–4.
[33] M.S. Kang, J.H. Kim, J.G. Won, S.H. Moon, Y.S. Kang, J. Membr. Sci. 247 (2005) 127–135.
[34] M.S. Kang, Y.J. Choi, S.H. Moon, J. Membr. Sci. 207 (2002) 157–170.
[35] C. Rocchiccioli-Deltcheff, R. Thouvenot, R. Franck, Spectrochim. Acta 32 (1976) 587–597.
[36] S. Shanmugam, B. Viswanathan, T.K. Varadarajan, J. Membr. Sci. 275 (2006) 105–109.
[37] H. Wang, B.A. Holmberg, L. Huang, Z. Wang, A. Mitra, J.M. Norbeck, Y. Yan, J. Mater. Chem. 12 (2002) 834–837.
[38] J.L. Souquet, M. Duclot, M. Levy, Solid State Ionics 85 (1996) 149–157.
[39] I. Honma, H. Nakajima, O. Nishikawa, T. Sugimoto, S. Nomura, Solid State Ionics 162/163 (2003) 237–245.
[40] J. Kim, T. Mori, I. Honma, J. Electrochem. Soc. 153 (2006) A508–A514.